THE JOURNAL OF BIOLOGICAL CHEMISTRY VOL. 283, NO. 22, pp. 14915–14926, May 30, 2008
Printed in the U.S.A.

ASAP3 Is a Focal Adhesion-associated Arf GAP That Functions in Cell Migration and Invasion*[S]

Received for publication, November 28, 2007, and in revised form, April 1, 2008 Published, JBC Papers in Press, April 8, 2008, DOI 10.1074/jbc.M709717200

Vi Luan Ha[‡], Sanita Bharti[‡], Hiroki Inoue[‡], William C. Vass[§], Fanny Campa[‡], Zhongzhen Nie[‡1], Armand de Gramont[¶], Yvona Ward[‖], and Paul A. Randazzo[‡2]

From the [‡]Laboratory of Cellular and Molecular Biology and [§]Laboratory of Cellular Oncology, [‖]Cell and Cancer Biology Branch, Center for Cancer Research, NCI and [¶]NIDDK, National Institutes of Health, Bethesda, Maryland 20892

ASAP3, an Arf GTPase-activating protein previously called DDEFL1 and ACAP4, has been implicated in the pathogenesis of hepatocellular carcinoma. We have examined *in vitro* and *in vivo* functions of ASAP3 and compared it to the related Arf GAP ASAP1 that has also been implicated in oncogenesis. ASAP3 was biochemically similar to ASAP1: the pleckstrin homology domain affected function of the catalytic domain by more than 100-fold; catalysis was stimulated by phosphatidylinositol 4,5-bisphosphate; and Arf1, Arf5, and Arf6 were used as substrates *in vitro*. Like ASAP1, ASAP3 associated with focal adhesions and circular dorsal ruffles. Different than ASAP1, ASAP3 did not localize to invadopodia or podosomes. Cells, derived from a mammary carcinoma and from a glioblastoma, with reduced ASAP3 expression had fewer actin stress fiber, reduced levels of phosphomyosin, and migrated more slowly than control cells. Reducing ASAP3 expression also slowed invasion of mammary carcinoma cells. In contrast, reduction of ASAP1 expression had no effect on migration or invasion. We propose that ASAP3 functions nonredundantly with ASAP1 to control cell movement and may have a role in cancer cell invasion. In comparing ASAP1 and ASAP3, we also found that invadopodia are dispensable for the invasive behavior of cells derived from a mammary carcinoma.

Cell migration is important to physiological processes such as development and inflammation and disease processes such as the invasion of normal tissue by cancer cells. Migration requires several temporally and spatially coordinated changes in the cellular membranes and cytoskeleton. Dynamic structures critical to cell movement include actin stress fibers, focal adhesions (FA),[3] circular dorsal ruffles (CDRs), and invadopodia (for reviews, see Refs. 1–7). Arf family GTP-binding proteins and Arf GTPase-activating proteins (GAPs) control these cytoskeletal structures (8–10). The molecular mechanisms by which Arf and Arf GAP proteins are spatially and temporally controlled and by which they interact with other regulatory elements are being discovered.

The Arfs are GTP-binding proteins (11–15). Six mammalian Arf proteins have been identified, five in the human genome. These are divided into 3 classes: class 1 includes Arfs 1–3; class 2 includes Arfs 4 and 5; class 3 includes Arf6. Class 1 and 3 Arf proteins have been examined more extensively than class 2 Arfs. Arf1 has been found to affect membrane traffic at the Golgi apparatus and in the endocytic compartment and to recruit paxillin to focal adhesions (12, 13). Arf6 has also been found to affect membrane traffic and the actin cytoskeleton including FAs and invadopodia (11, 16–19). The function of both Arf1 and Arf6 is dependent on the binding and hydrolysis of GTP, which is catalyzed by guanine nucleotide exchange factors and GAPs (8, 10, 13, 20).

The Arf GAPs are a family of multidomain proteins with the common catalytic function of accelerating the hydrolysis of GTP bound to Arf (8, 10, 20–22), thereby inactivating Arf proteins. The family can be subdivided based on domain structure. The AZAP group has a catalytic core of pleckstrin homology (PH), Arf GAP, and ankyrin repeat domains. Within this group, the ASAPs, ACAPs, AGAPs, and ARAPs have additional domains defining the subtypes. In addition to the PH, Arf GAP, and ankyrin repeat domains, ASAPs contain BAR, proline-rich, and SH3 domains; ACAPs have a BAR domain; AGAPs have a GTP-binding protein-like domain; the ARAPs have sterile α motif, 5 PH, Rho GAP, and Ras-association domains. Most Arf GAPs have been found to regulate cytoskeletal structures including FAs, CDRs, and invadopodia (for reviews see Refs. 8–10, 19, and 21–32). At least part of the molecular mechanism by which the different Arf GAPs affect actin involves the catalytic GTPase-activating protein activity. For instance, the Arf6-GAP activity of ARAP2 is required for formation of FAs (19). However, the multidomain Arf GAPs have additional functions. ASAP1 is an example of an Arf GAP that functions as a GTPase-activating protein and as a scaffold to regulate FAs and invadopodia (9, 26, 27, 33, 34).

* This work was supported, in whole or in part, by a National Institutes of Health grant from the Intramural Research Program (NCI), Department of Health and Human Services. The costs of publication of this article were defrayed in part by the payment of page charges. This article must therefore be hereby marked "*advertisement*" in accordance with 18 U.S.C. Section 1734 solely to indicate this fact.

[S] The on-line version of this article (available at http://www.jbc.org) contains supplemental Fig. S1.

[1] Current address: Dept. of Pathology, Medical College of Georgia, 1120 15th St., Augusta, GA 30912.

[2] To whom correspondence should be addressed: Bldg. 37, Rm. 2042, Bethesda, MD 20892. Tel.: 301-496-3788; Fax: 301-480-1260; E-mail: Randazzo@helix.nih.gov.

[3] The abbreviations used are: FA, focal adhesions; LUV, large unilamellar vesicles; DDEFL1, development and differentiation enhancing factor like-1; GST, glutathione *S*-transferase; CDR, circular dorsal ruffles; GAP, GTPase-activating protein; UPLC1, up-regulated in liver cancer 1; PH, pleckstrin homology; MLC, myosin light chain; siRNA, small interfering RNA; PBS, phosphate-buffered saline; MTT, 3-(4,5-dimethylthiazol-2-yl)-2,5-diphenyltetrazolium bromide; PI, phosphatidylinositol; PI(4)P, phosphatidylinositol 4-phosphate; $PI(4,5)P_2$, phosphatidylinositol 4,5-bisphosphate; $PI(3,4,5)P_3$, phosphatidylinositol 3,4,5-trisphosphate.

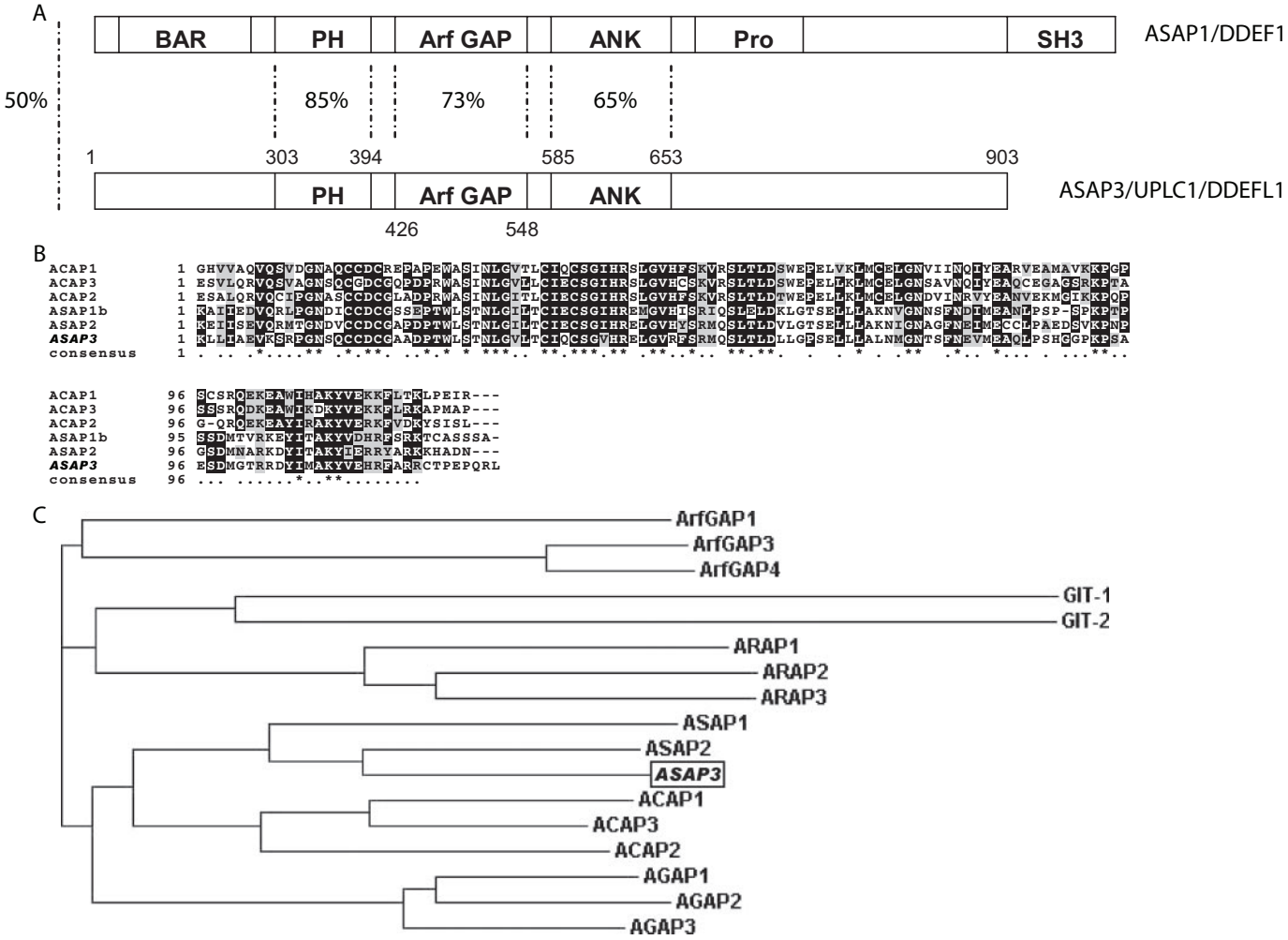

FIGURE 1. **UPLC1 is an ASAP-type protein.** *A*, schematic diagram of ASAP1 and ASAP3 domains. The structure of ASAP1 and ASAP3 was identified using on-line data bases of conserved protein domains (SMART and Pfam). Amino acid sequence similarity between the full-length proteins and each domain is indicated in percentages. *B*, alignment of Arf GAP domains using ClustalW. The *CXXC CXXC* motif representing the zinc finger is completely preserved. *C*, Arf GAP family phylogram. The phylogram was obtained from the multiple sequence alignment. The branch lengths in the phylogram are proportional to the estimated divergence along each branch. Accession numbers for human Arf GAPs are: ArfGAP1, NM_018209; ArfGAP3, NM_014570; ArfGAP4, NM_032389; Git1, NM_014030; Git2, NP_476510; ASAP1, BAA86563; ASAP2, NM_003887; ASAP3, NM_017707; ACAP1, NM_014716; ACAP2, NM_012287; ACAP3, NM_030649; AGAP1, NM_014770; AGAP2, NM_014914; AGAP3, NM_031946; ARAP1, NM_015242; ARAP2, NM_015230; ARAP3, NM_022481.

ASAP proteins are a subtype of Arf GAPs that have been implicated in oncogenesis. Three ASAP-type proteins have been identified so far. ASAP1 and ASAP2, but not ASAP3, contain an SH3 domain at the extreme C terminus (35, 36). The gene for ASAP1 is amplified in uveal melanoma and expression levels of ASAP1 have been found to correlate with invasive potential in uveal melanoma and mammary carcinoma (34, 37). In addition, ASAP1 associates with and regulates FAs, CDRs, and invadopodia/podosomes (26–28, 34, 38), structures involved in cell migration and invasion (2, 3, 39–41). Reducing ASAP1 expression has been reported to slow cell migration in some studies (25, 34), accelerate cell migration in others (26, 33), and decrease cell invasion (34).

ASAP3, previously called up-regulated in liver cancer 1 (UPLC1), DDEFL1 and ACAP4 (42, 43), was identified in analyses of expression profiles of clinical hepatocellular carcinomas using cDNA microarray. The relative expression of ASAP3 was high in hepatocellular carcinoma (43). The expression level of ASAP3 correlated with cell proliferation and migration (42). However, the localization of endogenous protein and the precise site of action have not been examined.

Here we characterize ASAP3 and test the hypothesis that ASAP3 and ASAP1, with highly similar structures, have redundant cellular functions in controlling cell migration and invasion. Biochemically, ASAP3 is similar to ASAP1; however, examination of the cellular function of ASAP3 revealed differences from ASAP1. First, ASAP3 localized in FAs and CDRs but, different from ASAP1, ASAP3 was not found in invadopodia or podosomes, structures reported to mediate invasion of cancer cells. Second, reduction of ASAP3 expression did not prevent the formation of invadopodia or podosomes; in contrast, reduction of ASAP1 blocked the formation of invadopodia and podosomes (34, 38). Decreasing the expression level of ASAP3 reduced actin stress fibers. Third, reduction of ASAP3 expression levels slowed cell migration and invasion, whereas reduction of ASAP1 expression did not affect these activities. Based on our results, we conclude that ASAP3 and ASAP1 do not function redundantly but have distinct functions. At least for the

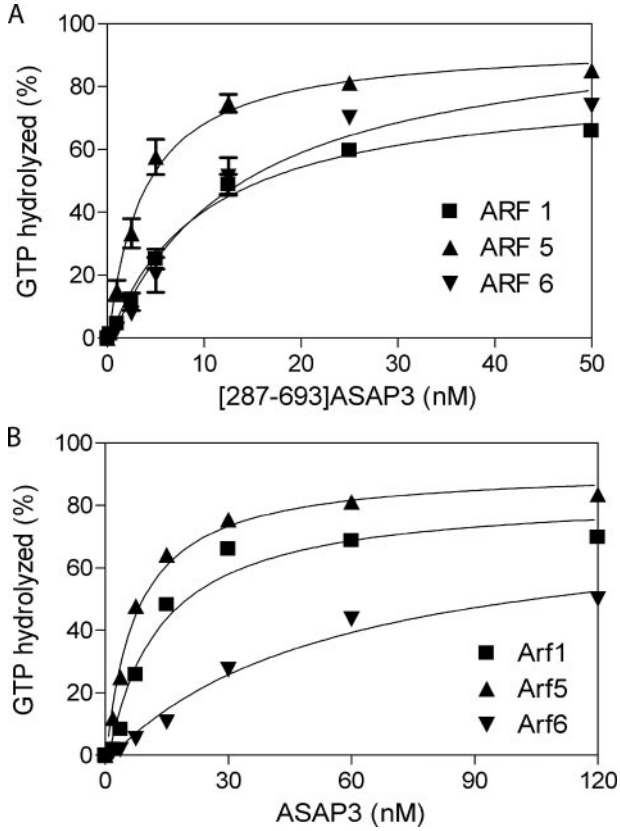

FIGURE 2. ***In vitro* Arf specificity of ASAP3.** The Arf GAP activity of the indicated proteins was determined using LUVs containing $PI(4,5)P_2$ with phosphatidylcholine, phosphatidylethanolamine, phosphatidylserine, PI, and cholesterol. Arf1, Arf5, and Arf6 at a concentration of 1 μM were used as representative members of class I, II, and III Arfs. *A*, [287–693]ASAP3. The *error bars* represent S.E.; $n = 3$. *B*, full-length ASAP3.

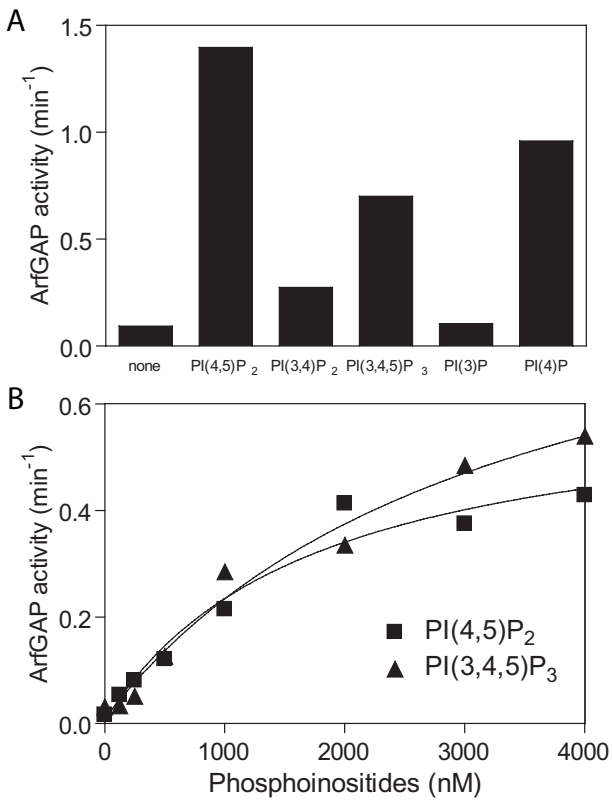

FIGURE 3. **Lipid dependence.** *A*, phosphoinositide specificity of Arf GAP activity of ASAP3. The Arf GAP activity was measured in the presence of 50 μM $PI(4,5)P_2$, 1 μM $PI(3,4)P_2$, 1 μM $PI(3,4,5)P_3$, 1 μM PI(3)P, and 50 μM PI(4)P. The activity of 2 nM full-length ASAP3 was determined using LUVs. Arf5 (1 μM) was used as the substrate. *B*, effects of phosphoinositides on the ASAP3 Arf GAP activity. The Arf GAP assay was performed in the presence of 2 nM purified full-length ASAP3, and LUVs supplemented with the indicated amount of phosphoinositides. Arf5 was used as the substrate.

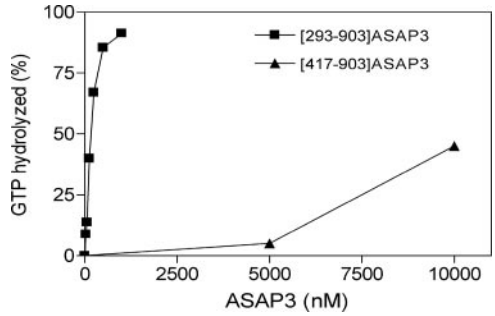

FIGURE 4. **PH domain of ASAP3 is required for efficient Arf GAP activity.** The Arf GAP assay was performed in the presence of mixed micelles of Triton X-100 containing 360 μM phosphatidic acid and 90 μM bovine brain $PI(4,5)P_2$. ASAP3 constructs [293–903] and [417–903] (construct lacking the PH domain) were titrated into the assay. Arf5 (1 μM) was used as a substrate.

mammary carcinoma cell line we examined, ASAP3 contributes to invasion but ASAP1 does not. Given the critical role of ASAP1 for invadopodia formation (38), these results also support the conclusion that invadopodia are dispensable for invasion.

EXPERIMENTAL PROCEDURES

Plasmids—Epitope-tagged (FLAG tag, hemagglutinin tag) of full-length ASAP3 (accession number NM_017707) and the GAP-deficient mutant ([R469K]ASAP3 and [R469A]ASAP3) were constructed in the mammalian expression vector pCI (Promega) with standard molecular biology procedures.

Antibodies—Rabbit antiserum against human ASAP3 was raised using a synthetic peptide WVISTEPGSDSEEDEEEKRC, residues 692–711 of ASAP3, conjugated to maleimide-activated keyhole limpet hemocyanin (Pierce) as an immunogen. Immunization was performed at BioWorld (Dublin, OH). The antiserum (Bio228) was affinity purified using an EZ-link kit from Pierce and used for this article (see supplemental materials and Fig. S1 for characterization). The other antibodies used in this study were as follows: mouse monoclonal anti-FLAG antibody M5 (Sigma; 1:1,000), rabbit anti-phosphomyosin light chain 2 (Ser^{19}), phospho-MLC2, (Cell Signaling, 1:1000), rabbit anti-myosin light chain 2 (MLC2) (Cell Signaling, 1:1000), rabbit polyclonal anti-hemagglutinin (Covance, 1:1,000), goat anti-rabbit IgG antibody conjugated with horseradish peroxidase (Bio-Rad, 1:3,000), goat anti-mouse IgG antibody conjugated with horseradish peroxidase (Bio-Rad, 1:3,000), Texas Red-conjugated goat anti-mouse IgG (Jackson ImmunoResearch, 1:200), fluorescein isothiocyanate-conjugated goat anti-rabbit IgG (Jackson ImmunoResearch, 1:200).

siRNA Preparation and Transfection—For RNA interference assays, 19-nucleotide small interfering RNA duplexes (siRNAs) with 3′-UU overhangs specific for the 3′-untranslated region (5′-3′) and the open reading frame ("Smart pool," combination of 4 siRNA duplexes) for human ASAP3/DDEFL1 (GenBank™ accession number NM_017707) were synthesized by Dharma-

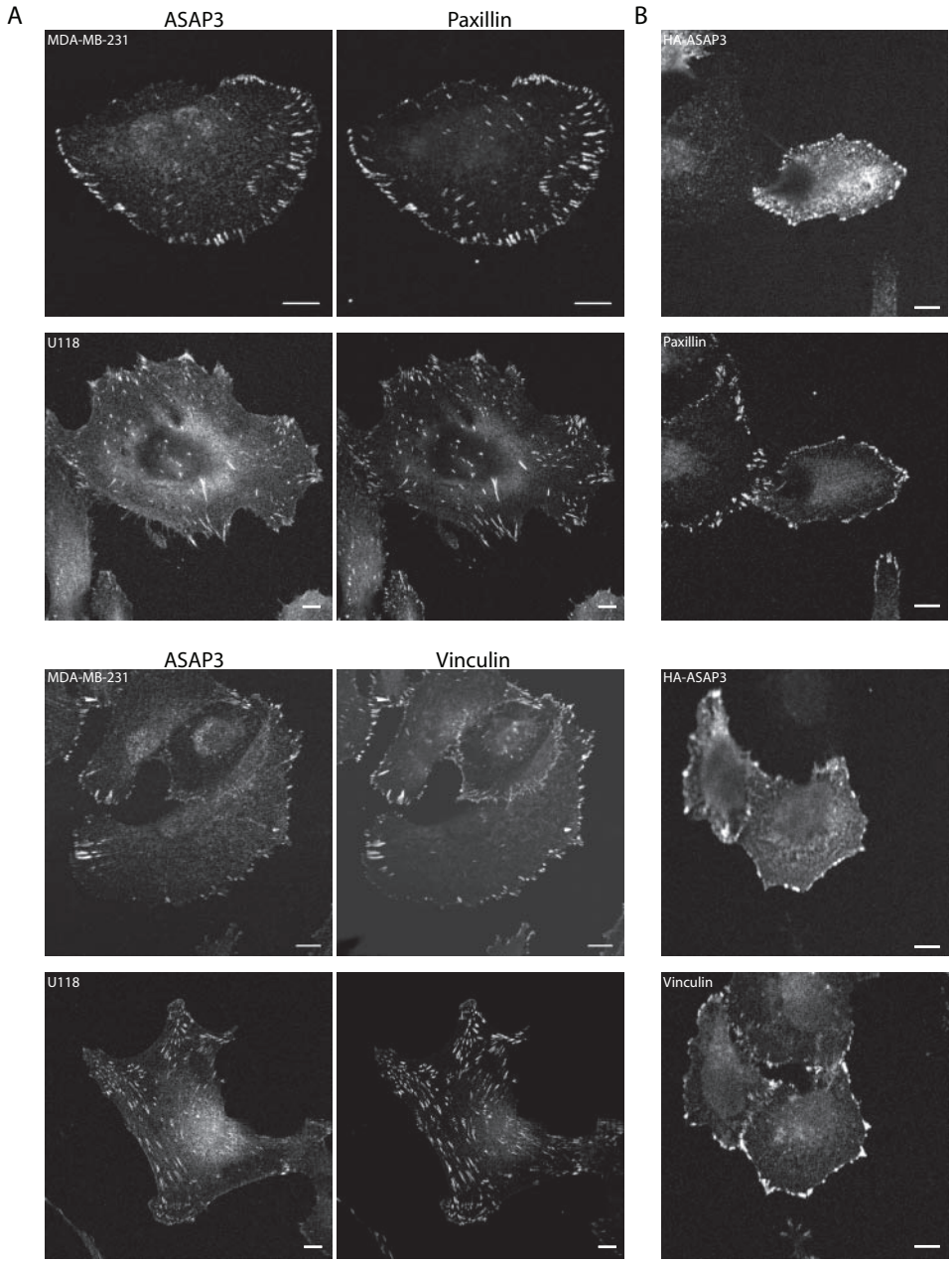

FIGURE 5. **Cellular distribution of ASAP3.** *A*, endogenous ASAP3 associates and colocalizes with markers of FAs. Antiserum 228 was used to detect endogenous ASAP3. Paxillin and vinculin were used as focal adhesion markers. *B*, epitope-tagged ASAP3. MDA-MB-231 cells expressing hemagglutinin-ASAP3 were fixed and stained for the hemagglutinin epitope and paxillin or vinculin. *Bars*, 10 μm.

con (Chicago, IL). The sequences were as follows: siRNA-1 sense, UCAGAUACCACACGAGUAAUU; siRNA-1 anti, UUACUCGUGUGGUAUCUGAUU; siRNA-2 sense, UAUAUGACCAUUACAGUUGUU; siRNA-2 anti, CAACUGUAAUGGUCAUAUAUU; siRNA-3 sense, GAAAGAAGGGAGAGUAAUAUU; siRNA-3 anti, UAUUACUCUCCCUUCUUUCUU; siRNA-4 sense, UCACUAAAUUCCAACUCUAUU; and siRNA-4 anti, UAGAGUUGGAAUUUAGUGAUU.

The siRNA duplexes used to target human ASAP1 (GenBank accession number NM_081482) specific for the open reading frame were synthesized by Invitrogen. The sequences were as follows: HSS147202, 5′-CCCAAAUUGGAGAUUUGCCGCCUAA-3′; HSS147203, 5′-GACCAGAUCUCUGUCUCGGAGUUCA-3′; and HSS147204, 5′-GGGCAAUAAGGAAUAUGGCAGUGAA-3′. The pool and individual siRNAs suppressed the expression of endogenous ASAP1 or ASAP3 efficiently (<80% knockdown assessed by Western blot analysis).

Silencer negative control number 2 siRNA (catalog D-001810-02-20) was purchased from Dharmacon. Cells were transfected with 100 nM siRNA using Lipofectamine 2000 (Invitrogen) transfection reagent according to the manufacturer's recommendations. The cells were harvested 48–96 h later and analyzed by Western blots and immunofluorescence.

Cell Culture and Cell Transfection—Human cell lines HepG2, U118, and MDA-MB-231 and mouse NIH 3T3 fibroblasts were maintained in Dulbecco's modified Eagle's medium supplemented with 10% heat-inactivated fetal bovine serum at 37 °C in a 5% CO_2 atmosphere at constant humidity.

Protein Expression and Purification from Bacteria—To express different constructs of ASAP3, reading frames for proteins of residues 287–693 (PZA), 1–693 (BAR-PZA), 417–903 (ZA-proline rich), 293–903 (ΔBAR ASAP3), and 1–903 (full-length ASAP3) of ASAP3 were ligated into the NdeI/XhoI sites of pET19b (Novagen), which contains a His_{10} fusion at the N terminus to express histidine-tagged proteins. Recombinant proteins were expressed in and purified from *Escherichia coli* over a HiTrap Q anion-exchange column (GE Healthcare) followed by a nickel affinity column (GE Healthcare) using gradients of NaCl and imidazole. Experiments were performed with the histidine-tagged proteins. Non-myristoylated Arfs were prepared as described (44).

Immunofluorescence—Cultured cells were seeded on fibronectin-coated coverslips for at least 4 h and fixed in 2% formaldehyde in phosphate-buffered saline (PBS) for 10 min at room temperature, washed three times with phosphate-buffered saline (PBS), and once in 10% fetal bovine serum and 0.04% sodium azide in PBS. Cells were then permeabilized in buffer A (10% fetal bovine serum, 0.04% sodium azide, and 0.2% saponin in PBS) for 10 min at room temperature. Cells were incubated with primary antibodies at 1:100 dilution in buffer A for 1 h at room temperature followed by incubation with appropriate

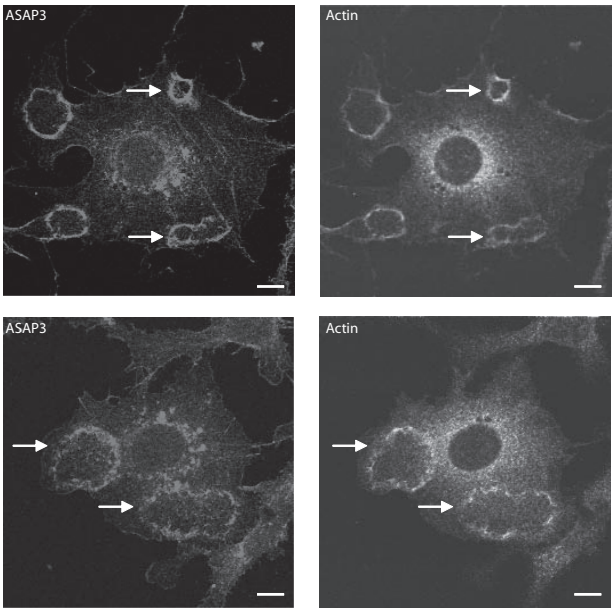

FIGURE 6. **ASAP3 localizes to circular dorsal ruffles in platelet-derived growth factor-treated NIH 3T3 stables overexpressing wild-type ASAP3.** Cells were treated with platelet-derived growth factor (10 ng/ml) for 5 min. Antiserum 228 was used to detect ASAP3 and polymerized actin was visualized with phalloidin conjugated to rhodamine. *Arrows* indicate CDRs. *Bars*, 10 μm.

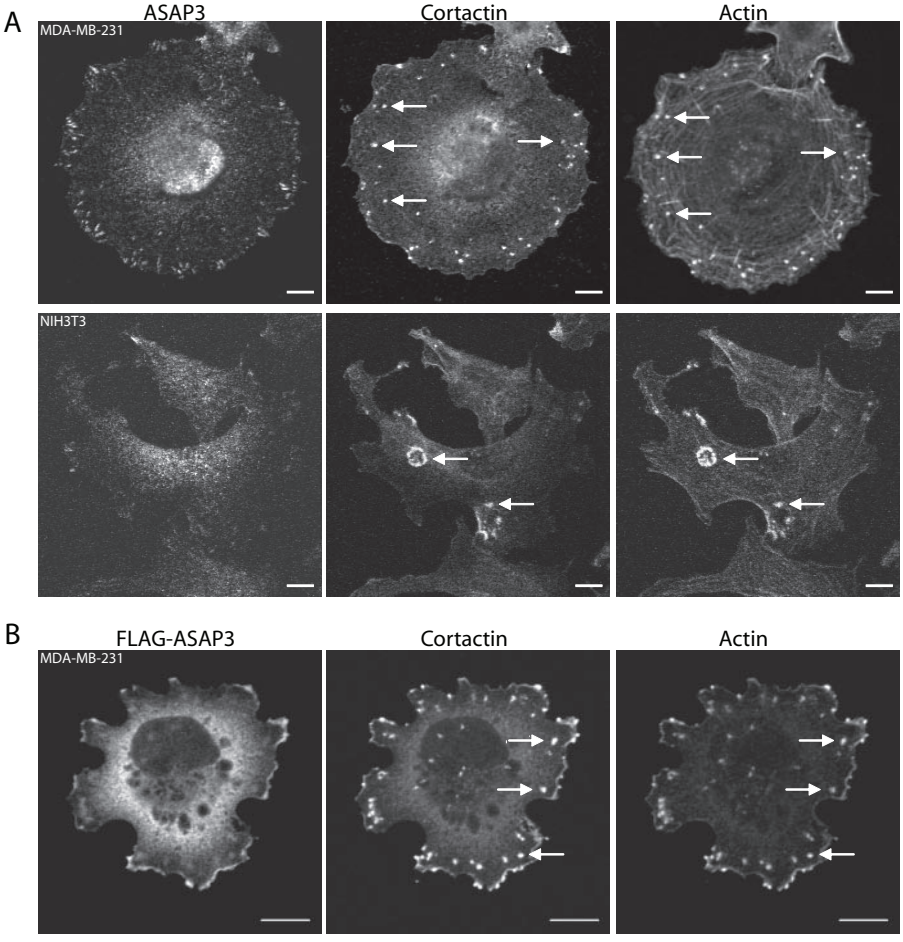

FIGURE 7. **ASAP3 does not associate with invadopodia or podosomes.** NIH3T3 fibroblasts or MDA-MB-231 cells were transfected with plasmids directing the expression of active Src([527F]c-Src) or plasmids directing the expression of FLAG-ASAP3. Invadopodia in MDA-MB-231 cells and podosomes in NIH3T3 fibroblasts were detected using actin or cortactin as markers. Antiserum 228 was used to detect endogenous ASAP3 (*A*) and anti-FLAG antibody was used to detect the recombinant ASAP3 (*B*). *Arrows* indicate invadopodia or podosomes. *Bars*, 10 μm.

secondary antibodies conjugated with fluorescein isothiocyanate (Jackson ImmunoResearch) for 1 h at room temperature. For visualization of actin filaments, rhodamine-conjugated phalloidin (Molecular Probes) was added during the incubation with secondary antibodies. Coverslips were then washed and mounted on glass slides with Gel Mount (Biomeda). Cells were visualized and images captured by confocal microscopy using a Zeiss LSM 510 attached to a Zeiss Axiovert 100M with a 63 × 1.4 NA plan Neofluar oil immersion lens. Adobe Illustrator was used to prepare the images for publication.

Western Blot Analysis—Cell lysates containing equivalents of total protein were resolved on a 10% SDS-polyacrylamide gel, followed by transfer to nitrocellulose membranes (Bio-Rad). Membranes were incubated in 4% nonfat dry milk for 1 h at room temperature, washed with PBS containing 0.1% Tween 20, followed by incubation with the primary antibody (as specified) for 1 h at room temperature or overnight at 4 °C. Membranes were then washed and incubated in the appropriate secondary antibody for 1 h at room temperature, and the immunocomplexes were visualized using ECL Plus Western blotting Detection System (Amersham Biosciences).

Cell Proliferation Assay—Cells treated with siRNA targeting ASAP3 or cells stably expressing ASAP3 or [R469K]ASAP3 were plated at a density of 20,000 cells per well in 12-well plates in 1 ml of culture medium containing 10% fetal bovine serum. Proliferation was monitored by counting cells each day using a hemocytometer. The experiments were repeated twice in triplicates each.

MTT Assay—Cells previously treated with the indicated siRNA were plated at a density of 3,000 cells per well in 96-well plates (200 μl/well) and incubated at 37 °C. MTT assay was performed every 24 h by adding 20 μl of MTT (5 mg/ml) 4 h before cell harvesting. The resulting MTT purple formazan crystals in each well were solubilized by addition of 100 μl of DMSO and absorbance was measured spectrophotometrically at a wavelength of 650 nm.

Wound Healing Assay—Monolayers of confluent cells were scratched with a sterile pipette tip and phase-contrast images of cells were taken either immediately after wounding or after 24 or 48 h. Repair of the artificial "wound" (% healing) was quantified as follows: healing (%) = ((1 − (width of wound at 0 h/width of wound at 24 or 48 h)) × 100.

Transwell Migration and Invasion Assay—Migration and invasion assays were carried out with cell cul-

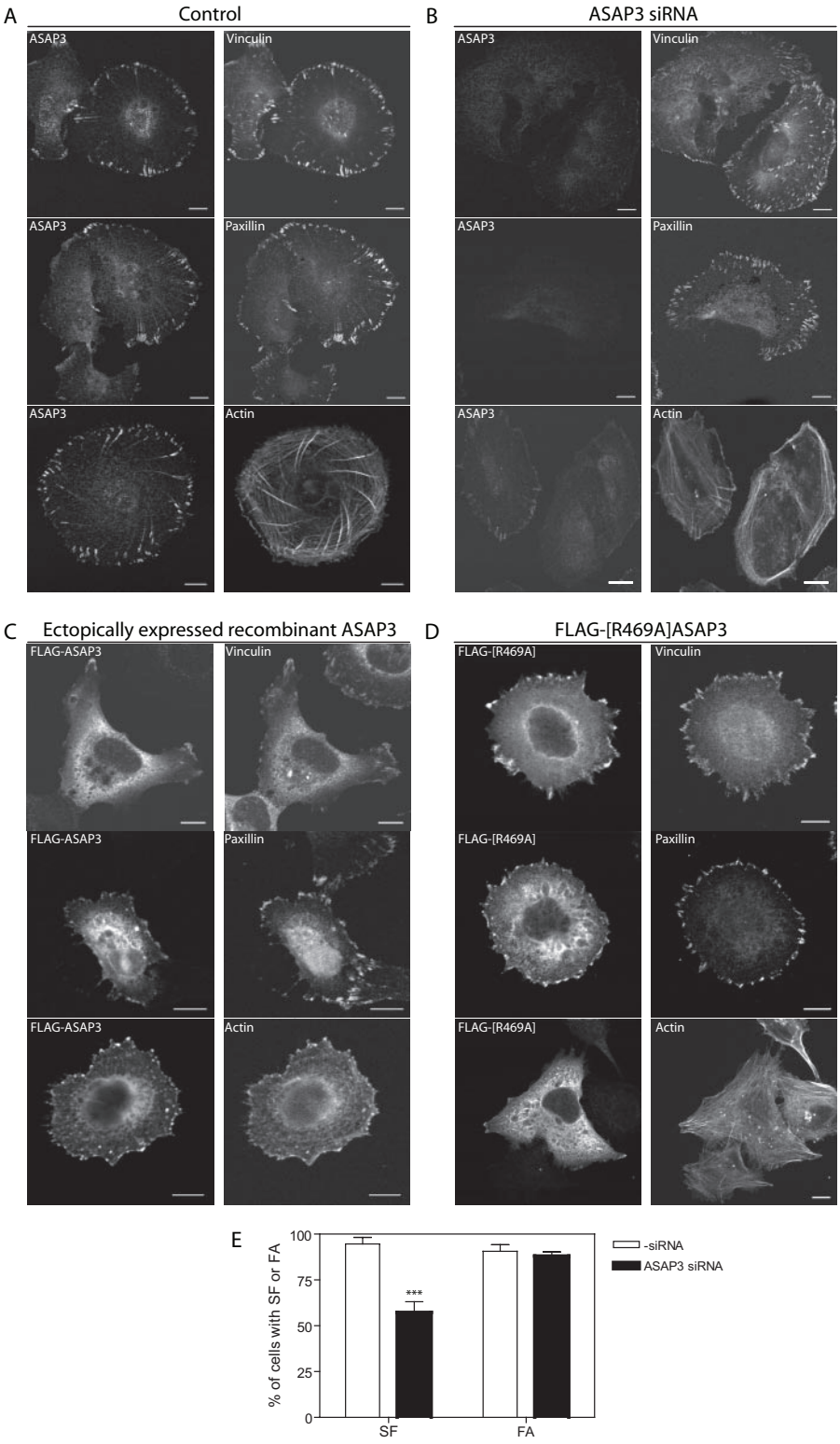

FIGURE 8. **Effects of ASAP3 on the cytoskeleton.** Untreated MDA-MB-231 cells (*A*), cells with reduced expression of ASAP3 (*B*), cells expressing epitope-tagged ASAP3 wild-type (*C*), or GAP-deficient mutant FLAG[R469A]ASAP3 (*D*) were seeded on fibronectin-coated coverslips, fixed, and stained for ASAP3 and vinculin, paxillin, or actin. *Bars*, 10 mm. *E*, quantification of the effects of ASAP3 knockdown on stress fibers (*SF*) and FA formation. MDA-MB-231 cells were treated with or without ASAP3 siRNA as indicated. Endogenous ASAP3 was detected using antiserum 228; filamentous stress fibers and focal adhesions were visualized with phalloidin conjugated to rhodamine and anti-vinculin antibody, respectively. At least 25 cells were counted from randomly chosen fields in triplicates for each experiment. *Error bars* represent S.E. *** indicates significantly different from non-transfected cells, $p < 0.001$.

ture inserts (8-μm pore size; BD Biosciences). For invasion assays, cell culture inserts were coated with 10 μg of Matrigel (BD Biosciences). The Matrigel was diluted in cold serum-free medium and added to the chambers and dried in a sterile hood for 4–5 h. The Matrigel was then reconstituted with serum-free medium for 1 h at 37 °C before the addition of cells.

Cells were harvested by trypsinization, resuspended in Opti-MEM and 1×10^4 cells were added to the upper chambers, and the chambers were placed in 24-well dishes. The lower compartment of the wells were filled with Dulbecco's modified Eagle's medium containing 10% fetal bovine serum used as chemoattractant. Migration assays were carried out for 12 h and invasion assays for 24 h. Cells were scraped off the top side of the polyethylene membrane with a cotton swab. Cells that invaded into the Matrigel and migrated out onto the lower surface of the membrane were stained in 0.2% crystal violet. Images of the cells that invaded the lower surface of the filter were taken with the ×2.5 objective of an inverted microscope (Nikon Eclipse E800) coupled to a digital camera (Hamamatsu C4742-95). Data were collected from at least three independent experiments each carried out in triplicate. Data are presented as percentages calculated by normalizing the values obtained for the cells treated with a negative control siRNA as 100%.

Site-directed Mutagenesis—Mutations were performed using the QuikChange kit (Stratagene) following the manufacturer's instructions and confirmed by DNA sequencing. Mutant proteins were purified as described above.

Arf GAP Assay—Arf GAP activity was determined using an *in vitro* assay that measures a single round of GTP hydrolysis on recombinant Arf (45, 46). Briefly, recombinant Arf proteins were preloaded with [α-^{32}P]GTP for 30 min at 37 °C. Purified ASAP3 proteins were added to GTP-loaded Arfs in the

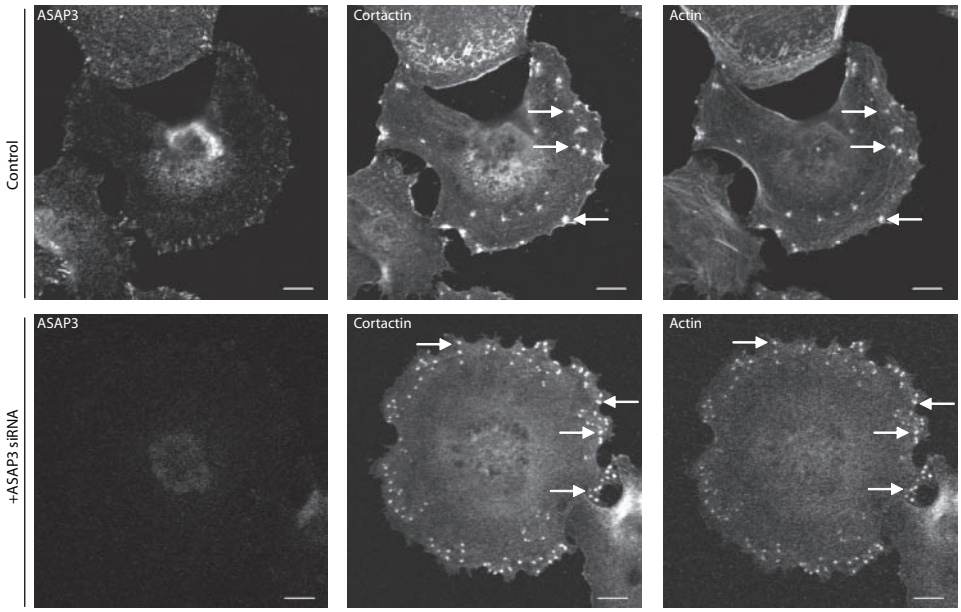

FIGURE 9. **Effects of reducing ASAP3 expression on the formation of invadopodia in MDA-MB-231 cells.** MDA-MB-231 cells previously treated with or without ASAP3 siRNA for 48 h were subsequently transfected with plasmids directing the expression of active Src([527F]c-Src). Under this condition, invadopodia were detected using actin or cortactin as markers. Antiserum 228 was used to detect endogenous ASAP3. *Arrows* indicate invadopodia. *Bars*, 10 μm.

presence of large unilamellar vesicles (LUVs). Reactions were terminated after 3 min by adding ice-cold buffer. Protein-bound nucleotide was trapped on nitrocellulose filters, released into formic acid, fractionated by chromatography on polyethyleneimide cellulose plates, and quantified using a PhosphorImager (GE Healthcare). All experiments were performed at least three times with similar results.

Preparation of Large Unilamellar Vesicles—Synthetic LUVs consisting of 40% phosphatidylcholine, 25% phosphatidylethanolamine, 15% phosphatidylserine, 9.5% phosphatidylinositol (PI), 0.5% phosphatidylinositol 4,5-bisphosphate ($PI(4,5)P_2$), and 10% cholesterol from liver or brain total lipid extracts (Avanti Polar Lipids) were obtained as follows. Lipids were dried under N_2 for >1 h and resuspended in phosphate-buffered saline for Arf GAP assays or in buffer containing 500 mM sucrose, 20 mM Hepes, pH 7.4, 20 mM KCl for lipid binding experiments. Lipids were regularly vortexed during a 10-min rehydration period. After rehydration, lipids were alternately frozen and thawed five times. Unilamellar liposomes were then formed by multiple passages (>10) through a Mini-Extruder (Avanti Polar Lipids) equipped with a 1-μm pore polycarbonate membrane (Avanti Polar Lipids).

Statistics—Numerical data are presented as the mean ± S.E. The data were analyzed by analysis of variance, followed by Dunnett's test to determine the statistical significance of differences. All statistical analyses were performed using GraphPad Prism for Windows version 4.0 (GraphPad).

RESULTS

Nomenclature

The protein we examine here was first called UPLC1. The protein was subsequently called development and differentiation enhancing factor like-1 (DDEFL1) because of similarity to ASAP1/DDEF1 (43) and ACAP4, because of similarity to ACAP subtype Arf GAPs (42). Computational analysis of the amino acid sequence of UPLC1/DDEFL1 identified common reported motifs such as the PH, Arf GAP, and ankyrin repeat domains (Fig. 1*A*). To determine the most appropriate name for the protein, we analyzed the primary sequence and phylogeny of the highly conserved Arf GAP domain of the reported mammalian Arf GAPs (Fig. 1, *B* and *C*). By both analyses, the protein first called UPLC1 is an ASAP-type protein and we, therefore, will refer to the protein as ASAP3. The deduced 903-amino acid sequence of ASAP3 showed 50% similarity with ASAP1 based on the analysis of the primary structure of the proteins.

Characterization of Enzymatic Properties

Arf Specificity—Arf1, Arf5, and Arf6 were used as representative members of class 1, 2, and 3 Arfs to determine specificity *in vitro* of ASAP3. A truncated form of ASAP3, containing PH, Arf GAP, and ankyrin repeat domains ([287–693]ASAP3) had 3–4-fold more activity against Arf5 than Arf1 and Arf6 measured by the hydrolysis of GTP bound to Arf (Fig. 2*A*) as described under "Experimental Procedures." Full-length ASAP3 had 2–3-fold greater activity against Arf5 than Arf1 and 10-fold greater activity against Arf5 than Arf6 (Fig. 2*B*).

Lipid Dependence—The PH domain of ASAP3 is similar to that of ASAP1, which has been found to specifically interact with $PI(4,5)P_2$. To characterize the interaction of ASAP3 with lipids, we determined the phosphoinositide dependence of GAP activity of ASAP3 using Arf5 as a substrate. Full-length ASAP3 was used as the enzyme in the experiments shown (Fig. 3). The data were similar to those obtained with two other PH domain-containing constructs such as [1–693]ASAP3 and [287–693]ASAP3. GAP activity was stimulated by phosphatidylinositol 4-phosphate (PI(4)P), $PI(4,5)P_2$, and $PI(3,4,5)P_3$ (Fig. 3*A*). Concentration dependence for $PI(4,5)P_2$ and $PI(3,4,5)P_3$ were similar (Fig. 3*B*). Given the relative cellular concentrations of $PI(4,5)P_2$ and $PI(3,4,5)P_3$, we conclude that $PI(4,5)P_2$ is the physiologically relevant activating lipid.

The dependence of GAP activity on the PH domain was also determined. [417–903]ASAP3, which lacks the PH domain, was compared with [293–903]ASAP3 in GAP assays (Fig. 4). In the presence of phosphoinositides, [417–903]ASAP3 had between 10^{-2} and 10^{-3} the activity of [293–903]ASAP3. Thus, the PH domain of ASAP3 is required for efficient catalytic activity of the protein.

Cellular Function of ASAP3

Localization—An antibody, raised, purified, and characterized as described under supplemental Materials, was used to

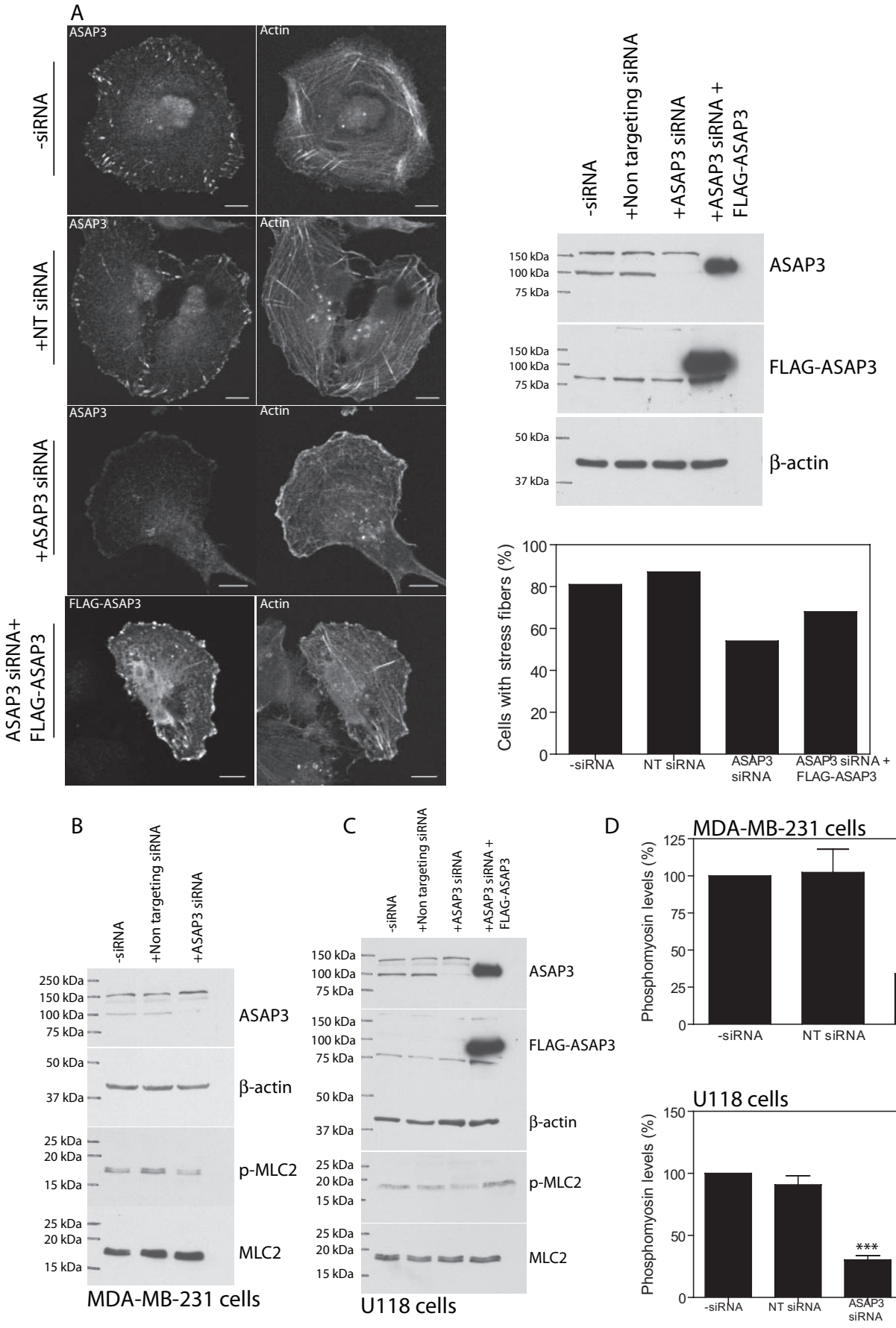
A
ASAP3
Actin
-siRNA
+NT siRNA
+ASAP3 siRNA
FLAG-ASAP3
ASAP3 siRNA+
FLAG-ASAP3
-siRNA
+Non targeting siRNA
+ASAP3 siRNA
+ASAP3 siRNA +
FLAG-ASAP3
150 kDa
100 kDa
75 kDa
ASAP3
FLAG-ASAP3
50 kDa
37 kDa
β-actin
Cells with stress fibers (%)
100
80
60
40
20
0
-siRNA
NT siRNA
ASAP3
siRNA
ASAP3 siRNA +
FLAG-ASAP3
B
-siRNA
+Non targeting siRNA
+ASAP3 siRNA
250 kDa
150 kDa
100 kDa
75 kDa
ASAP3
50 kDa
37 kDa
β-actin
25 kDa
20 kDa
15 kDa
p-MLC2
MLC2
MDA-MB-231 cells
C
-siRNA
+Non targeting siRNA
+ASAP3 siRNA
+ASAP3 siRNA +
FLAG-ASAP3
150 kDa
100 kDa
75 kDa
ASAP3
FLAG-ASAP3
50 kDa
37 kDa
β-actin
25 kDa
20 kDa
15 kDa
p-MLC2
MLC2
U118 cells
D
MDA-MB-231 cells
Phosphomyosin levels (%)
125
100
75
50
25
0
***
-siRNA
NT siRNA
ASAP3
siRNA
U118 cells
Phosphomyosin levels (%)
150
100
50
0
***
-siRNA
NT siRNA
ASAP3
siRNA
ASAP3 siRNA+
FLAG-ASAP3

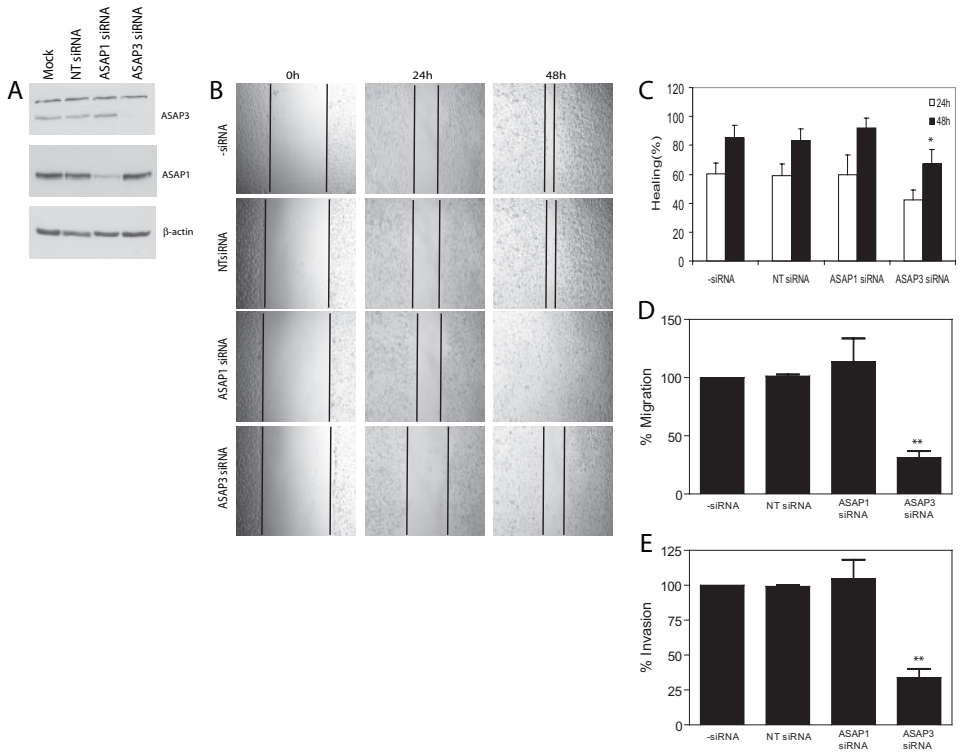

FIGURE 11. **Effect of ASAP3 on cell motility.** *A*, siRNA-mediated knockdown of ASAP1 and ASAP3 protein expression. Lysates prepared from siRNA-treated cells were analyzed by Western blotting using antibodies as indicated. *B*, migration on a surface. Representative example of six independent wound-healing assays at time 0, 24, and 48 h in MDA-MB-231 cells treated with non-targeting siRNA (*NT siRNA*, 100 nM) or siRNA targeting ASAP1 (*ASAP1 siRNA*, 100 nM) or siRNA targeting ASAP3 (*ASAP3 siRNA*, 100 nM). *C*, quantitative analyses of six independent wound-healing experiments. Data were analyzed by repeated measure analysis of variance followed by a Dunnett post test. * indicates significantly different from no siRNA control, $p < 0.05$. *D*, transwell migration. Cells treated as described in *B* were seeded in wells with membrane containing 8-μm pores. Twenty-four hours later, the cells migrating through the membrane were quantified. The *error bars* represent S.E.; $n = 6$. The data were analyzed as in *C*. ** indicates significantly different from non-targeting control, $p < 0.01$. *E*, migration through Matrigel. Experiment performed as in *D* with the Matrigel-coated membrane. The *error bars* represent S.E.; $n = 4$. The data were analyzed as in *C*. ** indicates significantly different from non-targeting control, $p < 0.01$.

determine the localization of ASAP3. ASAP3 was found to colocalize with two markers of FAs, vinculin and paxillin, in MDA-MB-231 (breast cancer) and U118 (glioblastoma) cells (Fig. 5*A*). Similarly, epitope-tagged ASAP3, expressed in MDA-MB-231 cells, associated with FAs (Fig. 5*B*).

We next determined whether ASAP3 also associated with CDRs and invadopodia. To visualize CDRs, NIH 3T3 fibroblasts, which stably expressed FLAG-ASAP3, were treated with platelet-derived growth factor. After 5 min, CDRs were detected as rings of polymerized actin on the dorsal surface of the cells. ASAP3 was found in the CDRs (Fig. 6). To visualize invadopodia in MDA-MB-231 cells and podosomes in NIH 3T3 fibroblasts, cells were transfected with plasmids expressing the active form of Src ([527F]c-Src). Under this condition, invadopodia and podosomes were detected, using actin or cortactin as markers, as punctate or ring-like structures on the ventral surface of the cell (Fig. 7). Endogenous ASAP3 (Fig. 7*A*) was not detected in either structure. Recombinant ASAP3 was also examined in MDA-MB-231 cells (Fig. 7*B*). It did not localize to invadopodia.

Effects of ASAP3 on the Cytoskeleton—We considered the possibility that ASAP3 affects the structure and function of FAs. As initial tests, recombinant ASAP3 was expressed to high levels in MDA-MB-231 cells. FAs were visualized with antibodies to paxillin and vinculin (Fig. 8*A*). In contrast to ASAP1 that causes dissociation of paxillin (26, 33), ASAP3 had no effect (Fig. 8*C*). [R469A]ASAP3, which does not have detectable GAP activity (data not shown), also did not affect the distribution of vinculin or paxillin (Fig. 8*D*). We also examined the effect of reducing ASAP3 expression, through the use of siRNA (Fig. 8, *B* and *E*). The protein level was reduced by 90% but no effect on the distribution of paxillin or vinculin was observed. We concluded that ASAP3 does not affect FAs under these conditions.

The effect of reduced ASAP3 expression on other cytoskeletal structures was examined. Invadopodia formation was not affected by reducing ASAP3 levels (Fig. 9). In the experiments examining focal adhesions (Fig. 8) and invadopodia (Fig. 9), polymerized actin was visualized with rhodamine-phalloidin. We noted that cells with reduced ASAP3 protein levels showed a disruption of the actin-containing stress fiber network compared with control cells (Figs. 8, *B* and *E*, 9, and 10). The effect

FIGURE 10. **Effects of ASAP3 on actin.** *A*, stress fibers. MDA-MB-231 cells treated with the indicated siRNA or mock transfected as a control for 48 h were subsequently transfected with FLAG-ASAP3 plasmids for another 24 h. Cells were then seeded onto fibronectin-coated slides, fixed, and stained with antiserum 228 to detect endogenous ASAP3, anti-FLAG antibodies to detect recombinant ASAP3, and rhodamine-phalloidin to visualize actin. *Bars* are 10 μm. The *left upper panel* shows ASAP3 protein levels in cells transfected with siRNA and siRNA-resistant plasmid. MDA-MB-231 cells were transfected with siRNA directed to the 3′-untranslated region of the ASAP3 message and plasmid directing expression of the indicated epitope-tagged proteins. Cells lysates were analyzed by Western blotting using antiserum 228 raised against ASAP3 and anti-FLAG antibody. The *left lower panel* shows the quantitation of the effects of reducing ASAP3 on stress fibers. At least 25 cells were counted from randomly chosen fields in triplicate for two experiments. *B*, effects of reducing ASAP3 expression on phospho-MLC2 levels. MDA-MB-231 cells were treated with siRNA to reduce ASAP3 expression or with non-targeting siRNA or mock-transfected as a control for 48 h. The cells were lysed and equal amounts of proteins were separated by PAGE. Endogenous ASAP3, β-actin, phospho-MLC2, and MLC2 levels were detected in total lysates with anti-ASAP3, anti-β-actin, anti-phospho-MLC2 (Ser^{19}), and anti-MLC2 antibodies. *C*, rescue of the effects ASAP3 siRNA-induced reduction of phosphomyosin levels. Rescue experiments were performed by transfecting the plasmid construct expressing FLAG-tagged wild-type ASAP3 in U118 cells 24 h after siRNA transfection. *D*, quantitation of effect on phosphomyosin. The *bar graphs* show the densitometric analysis using Scion Image software of three independent experiments. The *error bars* represent S.E.; $n = 3$ for MDA-MB-231, $n = 6$ for U118. *** indicates significantly different from non-targeting control, $p < 0.001$.

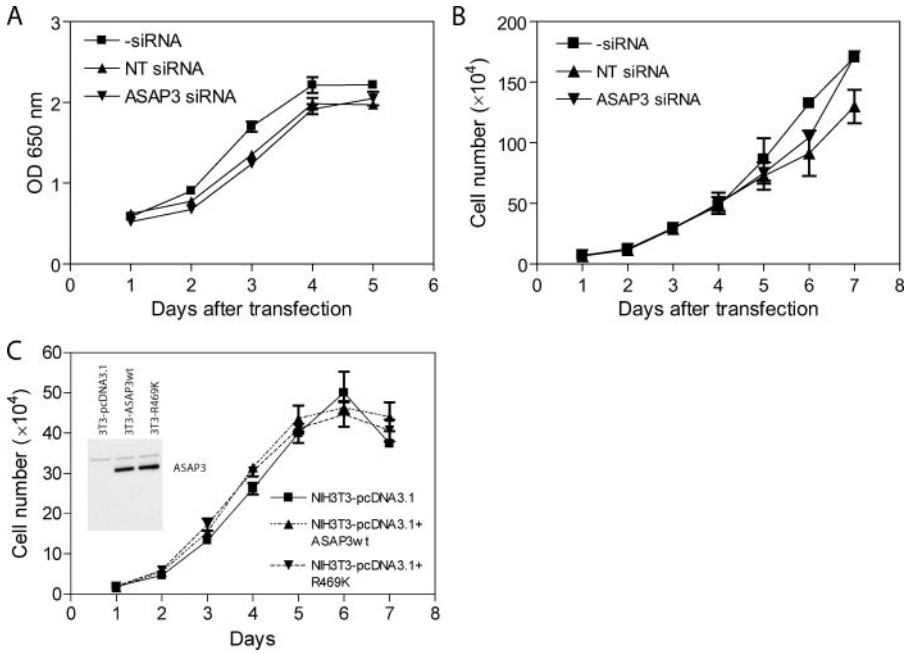

FIGURE 12. **Effect of ASAP3 on cell proliferation.** *A*, cell mass determined by MTT assay. MDA-MB-231 cells were treated with either ASAP3 siRNA or non-targeting siRNA or mock-transfected as a control for 48 h and were subsequently plated at a density of 3,000 cells/well in 96-well plates. MTT assay was performed every 24 h as described under "Experimental Procedures." *B*, growth of siRNA-treated MDA-MB-231 cells. Cells were seeded in 12-well plates. Cell number was determined using a hemocytometer as described under "Experimental Procedures." *C*, growth of NIH 3T3 fibroblasts expressing ASAP3 and [R469K]ASAP3. The experiment was performed as in *B*. *Error bars* represent S.E.

was independent of the siRNA used to reduce ASAP3. Stress fibers in MDA-MB-231 cells could be partly restored by expressing ASAP3 from a plasmid that was resistant to the siRNA-mediated silencing of ASAP3 (Fig. 10*A*).

Myosin phosphorylated on threonine 18 and serine 19 associates with and stabilizes actin stress fibers (4). We determined whether reduction of ASAP3 expression also affects phosphomyosin levels. In these experiments we examined both MDA-MB-231 and U118 cells. In both cell types, reduction of ASAP3 with siRNA resulted in decreased levels of myosin phosphorylated on serine 19 (Fig. 10, *B–D*). Phosphomyosin levels were restored if endogenous protein were replaced with recombinant ASAP3 by expression using an siRNA-resistant plasmid in U118 cells (Fig. 10, *C* and *D*). Taken together, our results support the conclusion that ASAP3 does not affect the structure of FAs but alters actin stress fibers that are associated with FAs.

Effects of ASAP3 on Cell Migration—We next examined whether ASAP3 affects cell migration. Treatment of MDA-MB-231 cells by ASAP3 siRNA suppressed the ASAP3 protein level by over 90% (Fig. 11*A*). Cell migration was examined in two ways. In a wound healing assay (Fig. 11, *B* and *C*), a monolayer of cells was scratched with a pipette tip, scraping cells from the surface. The movement of the cells into the artificial wound was observed over the course of 48 h. ASAP1 has previously been shown to affect cell migration (25, 26, 33) and was used as a control. We found that MDA-MB-231 with reduced ASAP1 migrated into the wound at the same rate as cells treated with an irrelevant siRNA. In contrast, reducing expression of ASAP3 reduced cell migration. Similar results were obtained using siRNA targeting a different sequence in the ASAP3 message.

Cell migration was also assessed using a transwell assay (Fig. 11*D*). As with the wound healing assay, MDA-MB-231 cells with reduced expression of ASAP3 migrated less than control cells; in contrast, reducing ASAP1 expression had no effect. Cell invasion involves migration through an extracellular matrix. To determine whether ASAP3 contributed to invasion, we used a MDA-MB-231 mammary carcinoma cells as a model and migration through Matrigel as an assay. Cells treated with siRNA targeting ASAP3 invaded less than cells treated with an irrelevant siRNA or untreated cells. The effect was independent of the particular targeting siRNA used. Although ASAP1 has been reported to be required for the formation of invadopodia (34, 38) and to be required for invasion (34), we found that the reduction of ASAP1 expression had no effect on invasion through Matrigel (Fig. 11*E*).

Role of ASAP3 in Cell Proliferation—Increased expression levels of ASAP3 have been reported to accelerate the proliferation of NIH 3T3 fibroblasts (44). To determine whether ASAP3 affects proliferation of other cell types, MDA-MB-231 cells were treated with siRNA targeting ASAP3 or an irrelevant RNA and cultured up to 7 days. In one assay, cell mass was determined with the MTT reagent. No difference between the cells treated with siRNA targeting ASAP3 and those treated with irrelevant RNA was observed (Fig. 12*A*). As a second measure of cell proliferation, cell number was determined using a hemocytometer. No differences in growth rates were observed (Fig. 12*B*). In a similar experimental design, NIH 3T3 fibroblasts stably expressing ASAP3 or [R469K]ASAP3 were seeded at subconfluent levels and grown for 7 days. No differences in the rate of cell proliferation were observed (Fig. 12*C*). Taken together, our data suggest that ASAP3 does not promote cell proliferation.

DISCUSSION

ASAP3 was first identified as a protein that contributes to cell proliferation in hepatocellular carcinoma and was later reported to be an Arf6-specific Arf GAP that regulates cell migration (42, 43). We set out to test whether ASAP3 functions redundantly with an Arf GAP of the same class, ASAP1, which has been implicated in the same processes. We found that, like ASAP1, ASAP3 associates with FAs and CDRs. However, ASAP3 was different from ASAP1 in two respects. First, ASAP3 was not found in nor was required for the formation of invadopodia. Second, reduction of ASAP3 levels reduced both cell migration and invasion rates, whereas reduction of ASAP1 had no detectable effect on invasion or migration. We conclude on

the basis of these results that ASAP1 and ASAP3 function non-redundantly in the control of cell movement.

One unexpected result of this work was that reduction of ASAP1 expression did not slow cell invasion, whereas reduction in ASAP3 did. Cells with reduced ASAP1 expression do not form invadopodia (38, 47), which are thought to mediate invasion. It is possible that the cells formed invadopodia-like structures with equivalent function, which we did not detect. Nevertheless, these results support the idea that invadopodia, as currently defined, are not necessary for invasion through Matrigel. Cells with reduced ASAP3 did form invadopodia, but did not invade efficiently. Thus, invadopodia are not sufficient for invasion.

Cells with reduced ASAP3 expression had less filamentous actin, consistent with current paradigms that ascribe a role for actin filaments in cell movement (48–52). With the decrease in actin stress fibers, there was less phosphomyosin. ASAP3 is found in FAs, which are complexes of proteins that attach to actin stress fibers. FAs and actin stress fibers are coordinately regulated, but some recent evidence supports the idea that they can be individually controlled. ARAP2, another Arf GAP found in FAs appears to be a Rho effector that regulates the formation of FAs (19). Reduction of ARAP2 expression blocks FA and stress fiber formation. Stress fibers, but not FAs, can be recovered by expression of activated Rho kinase. Thus, ARAP2 appears to have a greater influence on FA than stress fibers. Here we found that reduction of ASAP3 does not affect FA formation, but does disrupt filamentous actin. Based on these results, we conclude that Arf GAPs with a common localization could have independent functions. Ongoing work is focused on defining the molecular basis for cytoskeletal effects specific to different FA-associated Arf GAPs.

Arf GAPs can affect actin polymerization by a number of mechanisms (10), which may be relevant to ASAP3. For instance, Arf GAPs can interface with the Rho pathway. One class of Arf GAPs, called Gits, bind to PIX, a Rac/Cdc42 exchange factor, and p21 activated kinase (PAK), a Rac effector (22, 31, 32, 53). Another class of Arf GAPs, the ARAPs, contain Rho GAP domains (19, 54–58) and affect actin by converting RhoA·GTP to RhoA·GDP. Arf GAPs may also affect actin by regulating Arf proteins. Arf6, for instance, has been found to regulate a Rac exchange factor (59) and the trafficking of Rac1 (60, 61). Arf6 has also been reported to bind directly to Rac1 (62). Identification of associating proteins may reveal if any of these mechanisms apply to ASAP3.

The differential effects of ASAP1 and ASAP3 could be consequent to differences in Arf specificity. The Arf specificity of ASAP1 has not been clearly established. Several lines of evidence support the conclusion that ASAP1 is an Arf1 or Arf5 GAP (25, 26, 33, 35) but ASAP1 has also been reported to use Arf6 as a substrate (9). Our *in vitro* experiments indicated ASAP3 has a small preference for Arf5 and Arf1 as compared with Arf6. However, our *in vivo* studies were not conclusive (not shown). Previous reports supported the idea that Arf6 is the preferred substrate *in vitro*; however, in that work, GST-tagged Arf was used as a substrate (42). Given that GST is 26 kDa and Arf has a mass of 20 kDa, the GST could have affected the structure of Arf. Based on prevailing models for Arf action in cell migration, Arf6 is predicted to be the substrate. Examining the possibility that the ASAPs differ in specificity for class 1 and class 2 Arfs will require an expanded analysis and development of new experimental strategies.

In contrast to previous work, we did not observe an effect of ASAP3 on cell proliferation. We used three assays. First, we used the MTT assay as a means to measuring changes in total cell mass. Second, growth curves were determined. We also examined thymidine incorporation that did not reveal effects of ASAP3 (data not shown). The previously observed effects were modest (43). We may have not detected the effect due to lack of sensitivity in our assays. In summary, ASAP3 was identified as an Arf GAP that may regulate cell migration associated with the invasion of normal tissue by cancer cells.

Acknowledgment—Deborah Copeland, Howard Hughes Medical Institute high school teacher program, helped with the initial reverse transcriptase-PCR screening for ASAP3.

REFERENCES

1. Brunton, V. G., MacPherson, I. R. J., and Frame, M. C. (2004) *Biochim. Biophys. Acta* **1692,** 121–144
2. Ayala, I., Baldassarre, M., Caldieri, G., and Buccione, R. (2006) *Eur. J. Cell Biol.* **85,** 159–164
3. Buccione, R., Orth, J. D., and McNiven, M. A. (2004) *Nat. Rev. Mol. Cell Biol.* **5,** 647–657
4. Pelligrin, S., and Mellor, H. (2007) *J. Cell Sci.* **120,** 3491–3499
5. Carragher, N. O., and Frame, M. C. (2004) *Trends Cell Biol.* **14,** 241–249
6. Webb, D. J., Parsons, J. T., and Horwitz, A. F. (2002) *Nat. Cell Biol.* **4,** E97–E100
7. Wehrle-Haller, B., and Imhof, B. A. (2002) *Trends Cell Biol.* **12,** 382–389
8. Randazzo, P. A., and Hirsch, D. S. (2004) *Cell. Signal.* **16,** 401–413
9. Sabe, H., Onodera, Y., Mazaki, Y., and Hashimoto, S. (2006) *Curr. Opin. Cell Biol.* **18,** 558–564
10. Randazzo, P. A., Inoue, H., and Bharti, S. (2007) *Biol. Cell* **99,** 583–600
11. Donaldson, J. G. (2003) *J. Biol. Chem.* **278,** 41573–41576
12. Donaldson, J. G., Honda, A., and Weigert, R. (2005) *Biochim. Biophys. Acta* **1744,** 364–373
13. Randazzo, P. A., Nie, Z., Miura, K., and Hsu, V. (2000) *Sci STKE* **59,** RE1
14. Moss, J., and Vaughan, M. (1998) *J. Biol. Chem.* **273,** 21431–21434
15. Logsdon, J. M., and Kahn, R. A. (2003) in *Arf family GTPases* (Kahn, R. A., ed) pp. 1–21, Kluwer Academic Publishers, Dordrecht
16. Hashimoto, S., Onodera, Y., Hashimoto, A., Tanaka, M., Hamaguchi, M., Yamada, A., and Sabe, H. (2004) *Proc. Natl. Acad. Sci. U. S. A.* **101,** 6647–6652
17. Sabe, H. (2003) *J. Biochem.* (*Tokyo*) **134,** 485–489
18. Palacios, F., and Souza-Schorey, C. (2003) *J. Biol. Chem.* **278,** 17395–17400
19. Yoon, H.-Y., Miura, K., Cuthbert, E. J., Davis, K. K., Ahvazi, B., Casanova, J. E., and Randazzo, P. A. (2006) *J. Cell Sci.* **119,** 4650–4666
20. Donaldson, J. G., and Jackson, C. L. (2000) *Curr. Opin. Cell Biol.* **12,** 475–482
21. Inoue, H., and Randazzo, P. A. (2007) *Traffic* **8,** 1465–1475
22. Turner, C. E., West, K. A., and Brown, M. C. (2001) *Curr. Opin. Cell Biol.* **13,** 593–599
23. de Curtis, I. (2001) *EMBO Rep.* **2,** 277–281
24. Turner, C. E., Brown, M. C., Perrotta, J. A., Riedy, M. C., Nikolopoulos, S. N., McDonald, A. R., Bagrodia, S., Thomas, S., and Leventhal, P. S. (1999) *J. Cell Biol.* **145,** 851–863
25. Furman, C., Short, S. M., Subramanian, R. R., Zetter, B. R., and Roberts, T. M. (2002) *J. Biol. Chem.* **277,** 7962–7969
26. Liu, Y. H., Loijens, J. C., Martin, K. H., Karginov, A. V., and Parsons, J. T. (2002) *Mol. Biol. Cell* **13,** 2147–2156
27. Oda, A., Wada, I., Miura, K., Okawa, K., Kadoya, T., Kato, T., Nishihara, H., Maeda, M., Tanaka, S., Nagashima, K., Nishitani, C., Matsuno, K.,

Ishino, M., Machesky, L. M., Fujita, H., and Randazzo, P. (2003) *J. Biol. Chem.* **278,** 6456–6460
28. Randazzo, P. A., Andrade, J., Miura, K., Brown, M. T., Long, Y. Q., Stauffer, S., Roller, P., and Cooper, J. A. (2000) *Proc. Natl. Acad. Sci. U. S. A.* **97,** 4011–4016
29. Amerongen, G. P. V., Natarajan, K., Yin, G. Y., Hoefen, R. J., Osawa, M., Haendeler, J., Ridley, A. J., Fujiwara, K., van Hinsbergh, V. W. M., and Berk, B. C. (2004) *Circ. Res.* **94,** 1041–1049
30. Frank, S. R., Adelstein, M. R., and Hansen, S. H. (2006) *EMBO J.* **25,** 1848–1859
31. Manabe, R., Kovalenko, M., Webb, D. J., and Horwitz, A. R. (2002) *J. Cell Sci.* **115,** 1497–1510
32. Zhao, Z. S., Manser, E., Loo, T. H., and Lim, L. (2000) *Mol. Cell. Biol.* **20,** 6354–6363
33. Liu, Y., Yerushalmi, G. M., Grigera, P. R., and Parsons, J. T. (2005) *J. Biol. Chem.* **280,** 8884–8892
34. Onodera, Y., Hashimoto, S., Hashimoto, A., Morishige, M., Yamada, A., Ogawa, E., Adachi, M., Sakurai, T., Manabe, T., Wada, H., Matsuura, N., and Sabe, H. (2005) *EMBO J.* **24,** 963–973
35. Brown, M. T., Andrade, J., Radhakrishna, H., Donaldson, J. G., Cooper, J. A., and Randazzo, P. A. (1998) *Mol. Cell. Biol.* **18,** 7038–7051
36. Andreev, J., Simon, J. P., Sabatini, D. D., Kam, J., Plowman, G., Randazzo, P. A., and Schlessinger, J. (1999) *Mol. Cell. Biol.* **19,** 2338–2350
37. Ehlers, J. P., Worley, L., Onken, M. D., and Harbour, J. W. (2005) *Clin. Cancer Res.* **11,** 3609–3613
38. Bharti, S., Inoue, H., Bharti, K., Hirsch, D. S., Nie, Z., Yoon, H. Y., Artym, V., Yamada, K. M., Mueller, S. C., Barr, V. A., and Randazzo, P. A. (2007) *Mol. Cell. Biol.* **27,** 8271–8283
39. Linder, S., and Aepfelbacher, M. (2003) *Trends Cell Biol.* **13,** 376–385
40. Spinardi, L., and Marchisio, P. C. (2006) *Eur. J. Cell Biol.* **85,** 191–194
41. Yamaguchi, H., Pixley, F., and Condeelis, J. (2006) *Eur. J. Cell Biol.* **85,** 213–218
42. Fang, Z. Y., Miao, Y., Ding, X., Deng, H., Liu, S. Q., Wang, F. S., Zhou, R. H., Watson, C., Fu, C. H., Hu, Q. C., Lillard, J. W., Powell, M., Chen, Y., Forte, J. G., and Yao, X. B. (2006) *Mol. Cell. Proteomics* **5,** 1437–1449
43. Okabe, H., Furukawa, Y., Kato, T., Hasegawa, S., Yamaoka, Y., and Nakamura, Y. (2004) *Int. J. Oncol.* **24,** 43–48
44. Randazzo, P. A., Weiss, O., and Kahn, R. A. (1992) *Methods Enzymol.* **219,** 362–369
45. Randazzo, P. A., and Kahn, R. A. (1994) *J. Biol. Chem.* **269,** 10758–10763
46. Luo, R., Ahvazi, B., Amariei, D., Shroder, D., Burrola, B., Losert, W., and Randazzo, P. A. (2007) *Biochem. J.* **402,** 439–447
47. Hashimoto, S., Hirose, M., Hashimoto, A., Morishige, M., Yamada, A., Hosaka, H., Akagi, K. I., Ogawa, E., Oneyama, C., Agatsuma, T., Okada, M., Kobayashi, H., Wada, H., Nakano, H., Ikegami, T., Nakagawa, A., and Sabe, H. (2006) *Proc. Natl. Acad. Sci. U. S. A.* **103,** 7036–7041
48. Petit, V., and Thiery, J. P. (2000) *Biol. Cell* **92,** 477–494
49. Ridley, A. J. (2001) *J. Cell Sci.* **114,** 2713–2722
50. Wozniak, M. A., Modzelewska, K., Kwong, L., and Keely, P. J. (2004) *Biochim. Biophys. Acta* **1692,** 103–119
51. Walker, J. L., Fournier, A. K., and Assoian, R. K. (2005) *Cytokine Growth Factor Rev.* **16,** 395–405
52. Chen, C. S., Tan, J., and Tien, J. (2004) *Ann. Rev. Biomed. Eng.* **6,** 275–302
53. Brown, M. C., Cary, L. A., Jamieson, J. S., Cooper, J. A., and Turner, C. E. (2005) *Mol. Biol. Cell* **16,** 4316–4328
54. Miura, K., Jacques, K. M., Stauffer, S., Kubosaki, A., Zhu, K. J., Hirsch, D. S., Resau, J., Zheng, Y., and Randazzo, P. A. (2002) *Mol. Cell* **9,** 109–119
55. I, S. S. T., Nie, Z. Z., Stewart, A., Najdovska, M., Hall, N. E., He, H., Randazzo, P. A., and Lock, P. (2004) *J. Cell Sci.* **117,** 6071–6084
56. Krugmann, S., Anderson, K. E., Ridley, S. H., Risso, N., McGregor, A., Coadwell, J., Davidson, K., Eguinoa, A., Ellson, C. D., Lipp, P., Manifava, M., Ktistakis, N., Painter, G., Thuring, J. W., Cooper, M. A., Lim, Z. Y., Holmes, A. B., Dove, S. K., Michell, R. H., Grewal, A., Nazarian, A., Erdjument-Bromage, H., Tempst, P., Stephens, L. R., and Hawkins, P. T. (2002) *Mol. Cell* **9,** 95–108
57. Krugmann, S., Andrews, S., Stephens, L., and Hawkins, P. T. (2006) *J. Cell Sci.* **119,** 425–432
58. Krugmann, S., Williams, R., Stephens, L., and Hawkins, P. T. (2004) *Curr. Biol.* **14,** 1380–1384
59. Koo, T. H., Eipper, B. A., and Donaldson, J. G. (2007) *BMC Cell Biol.* **8,** 29
60. Radhakrishna, H., Al-Awar, O., Khachikian, Z., and Donaldson, J. G. (1999) *J. Cell Sci.* **112,** 855–866
61. Balasubramanian, N., Scott, D. W., Castle, J. D., Casanova, J. E., and Schwartz, M. A. (2007) *Nat. Cell Biol.* **9,** 1381–1381
62. Cotton, M., Boulay, P. L., Houndolo, T., Vitale, N., Pitcher, J. A., and Claing, A. (2007) *Mol. Biol. Cell* **18,** 501–511